Measuring the Natural Fluorescence of Phytoplankton Cultures

S. R. LANEY,* R. M. LETELIER, R. A. DESIDERIO, AND M. R. ABBOTT

College of Oceanic and Atmospheric Sciences, Oregon State University, Corvallis, Oregon

D. A. KIEFER

Department of Biological Sciences, University of Southern California, San Diego, California

C. R. BOOTH

Biospherical Instruments Inc., San Diego, California

ABSTRACT

A laboratory instrument, the Natural Fluorescence Chemostat, was developed to measure the natural fluorescence of phytoplankton cultures. With this instrument, the physical and chemical environment of a culture can be manipulated with respect to temperature, pH, nutrient delivery rate, and light intensity, while the natural fluorescence and a weak stimulated fluorescence are continuously recorded with high temporal resolution. The geometry and spectral distribution of the artificial light field minimize the contribution of scattering to the natural fluorescence signal. Preliminary investigations with the marine diatom *T. weissflogii* (Bacillariophyceae) indicate that the instrument can detect natural fluorescence signals in broadband artificial light fields as bright as 1250 μmol quanta m^{-2} s^{-1}. Since the influence of environmental factors on natural fluorescence is not well understood, laboratory experiments are essential for investigating how ocean physics and chemistry influence this signal. This instrument provides a quantitative means to examine how the magnitude and kinetics of phytoplankton natural fluorescence vary in response to changes in the physical and chemical environment.

1. Introduction

a. Motivation

Photosynthetic organisms have evolved complex structures of pigments and proteins to absorb light energy within the visible range of wavelengths, the so-called photosynthetically active radiation (PAR) between approximately 400 and 700 nm. A fraction of this absorbed energy is not used for photosynthesis and instead is lost to the environment in the form of heat and light. At in vivo temperatures, the energy dissipated as light is emitted almost completely from chlorophyll *a* molecules organized in the photosynthetic structure called Photosystem II. This phenomenon is known as chlorophyll fluorescence and represents an optical signal unique to photosynthetic organisms.

With respect to phytoplankton exposed to a natural light field, this emission is often referred to as "sun-stimulated," "solar-induced," "natural," or "passive" fluorescence. For simplicity, we will reserve the term sun-stimulated specifically for situations in which fluorescence is excited by a solar ambient light field, and we will use natural for the more general phenomenon. Natural fluorescence will be evident whenever phytoplankton are present in a light field conducive to phytoplankton growth, whereas so-called active fluorescence occurs only by purposeful stimulation by intense, artificial light sources such as a laser in a LIDAR system or a light emitting diode in a fluorometer. Such intense excitation is designed to "overload" the photosynthetic apparatus of phytoplankton to maximize the resulting fluorescence signal. In contrast, natural "fluorometers" are actually radiometers, detecting the fluorescence emission from phytoplankton "under load" at natural irradiance levels. Issues such as measurement technique, quality and delivery rate of excitation, and physiological interpretation have led to significant debate in the oceanographic community regarding the relative merits and drawbacks of measuring these similar, but subtly different, fluorescence signals. The physiological interpretation of fluorescence has received particular attention (e.g., Kiefer and Reynolds 1992).

---

* Current affiliation: Darling Marine Center, University of Maine, Walpole, Maine.

Corresponding author address: Dr. Samuel R. Laney, Darling Marine Center, University of Maine, 193 Clark's Cove Road, Walpole, ME 04573.
E-mail: sam@hawkeye.dmc.maine.edu

In oceanographic research, in situ measurement of sun-stimulated fluorescence is increasingly becoming routine. Natural fluorometers are operationally attractive because they have lower power requirements than their active counterparts, which makes them suitable for deployment on long term drifters and moorings (Abbott and Letelier 1997a,b; 1998). Field measurements of sun-stimulated fluorescence have been used to estimate chlorophyll concentrations (Kiefer et al. 1989; Abbott and Letelier 1997b), instantaneous rates of photosynthesis (Kiefer et al. 1989; Chamberlin et al. 1990; Chamberlin and Marra 1992; Stegmann et al. 1992; Doerffer 1993), and ecological responses to environmental transients (Letelier et al. 1997; Abbott and Letelier 1998). Additionally, in situ measurement of sun-stimulated fluorescence radiance serves as a means to ground truth natural fluorescence radiometers on remote sensing platforms. Satellite sensors like the National Aeronautics and Space Administration's (NASA) Moderate Resolution Imaging Spectrometer (MODIS), the National Space Development Agency of Japan's Global Imager, and the European Space Agency's Medium Resolution Imaging Spectrometer can provide sensitive, near-global coverage of natural fluorescence on the basin scale (Letelier and Abbott 1996). Preliminary interpretation of MODIS fluorescence data suggests that substantial mesoscale variability occurs in the chlorophyll fluorescence efficiency (Abbott et al. 2000).

In contrast to the comparatively sizeable amount of sun-stimulated fluorescence observations, to the best of our knowledge no detailed laboratory studies of natural fluorescence have been published. Controlled experiments using phytoplankton cultures are essential for understanding how ocean physics and chemistry influence the quantum yield of natural fluorescence and thus how variability in environmental factors contribute to observed variability in sun-stimulated fluorescence data. Such factors include irradiance intensity, spectral quality, nutrient availability, and temperature, and culture experiments can be employed to investigate each of these independently. To date, laboratory investigations of natural fluorescence have been hindered by a lack of instrumentation suitable for measuring this signal given the limitations dictated by phytoplankton culturing techniques. To address the lack of adequate laboratory instrumentation, we obtained and redesigned a fluorescence monitoring prototype originally designed and built by Biospherical Instruments Inc. We refer to this system as the Natural Fluorescence Chemostat (NFC) and have used it to obtain detailed laboratory time series of natural fluorescence under tightly regulated environmental conditions.

b. Requirements

Three priorities were identified regarding the redesign of the prototype instrumentation. First, we wished to measure the natural fluorescence signal in phytoplank-

ton cultures with optical densities similar to those found in the oligotrophic ocean (i.e., chlorophyll concentrations ≈ 0.05 μg L^{-1}). Although natural fluorescence can be easily observed in phytoplankton cultures with higher chlorophyll concentrations, the optical properties and nutrient dynamics in such dense cultures do not necessarily approximate natural conditions. Second, we wished to measure this natural fluorescence over the range of irradiances that occur naturally in the euphotic zone. We are especially interested in dynamics at the very near surface (i.e., the upper 6–10 m) where irradiance intensity can exceed 2000 μmol quanta m^{-2} s^{-1} at solar noon on cloudless days. The physiological response to such high intensities has a substantial but poorly understood effect on natural fluorescence (Cullen and Lewis 1995). Since at these depths commercially available field instruments cannot discriminate natural chlorophyll fluorescence from Raman scattering or elastic scattering from water and/or particles (Kiefer et al. 1989; Hu and Voss 1998), natural fluorescence remains significantly undersampled at such light levels. Third, since variability in natural fluorescence can result from wavelength dependent changes in phytoplankton absorption, we wished to additionally monitor natural fluorescence as a function of excitation wavelength (i.e., the action spectrum of natural fluorescence). To accomplish this, a very weak active fluorescence must be stimulated within the culture vessel, but this stimulation may not in any way disturb the physiological and/or optical state of the culture.

2. System design

We obtained prototype equipment from prior work performed by Dr. Dale Kiefer (University of Southern California) and C. R. Booth (Biospherical Instruments, San Diego, California). The prototype was evaluated and reengineered to address our specific measurement requirements. Although some improvement resulted from innovations in optics and electronics in the elapsed decade since the prototype was initially fabricated, other improvements represent novel approaches to the laboratory measurement of natural fluorescence, especially with respect to the measurement protocol. The NFC comprises three major systems: an environmentally controlled culture vessel, a passive/active fluorescence detection and discrimination system, and a computerized data acquisition and control system (Fig. 1).

a. Chemostat system

Phytoplankton are grown inside the NFC in an upright Pyrex cylinder (vessel P, Fig. 1), 250 mm high by 110 mm in diameter, with a culture volume of approximately 2.5 L. The nutrient delivery rate is controlled by a variable speed peristaltic manifold pump (Insmatec Reglo, pump BB, Fig. 1), and so although we refer to this instrument as a "chemostat," implying a constant rate
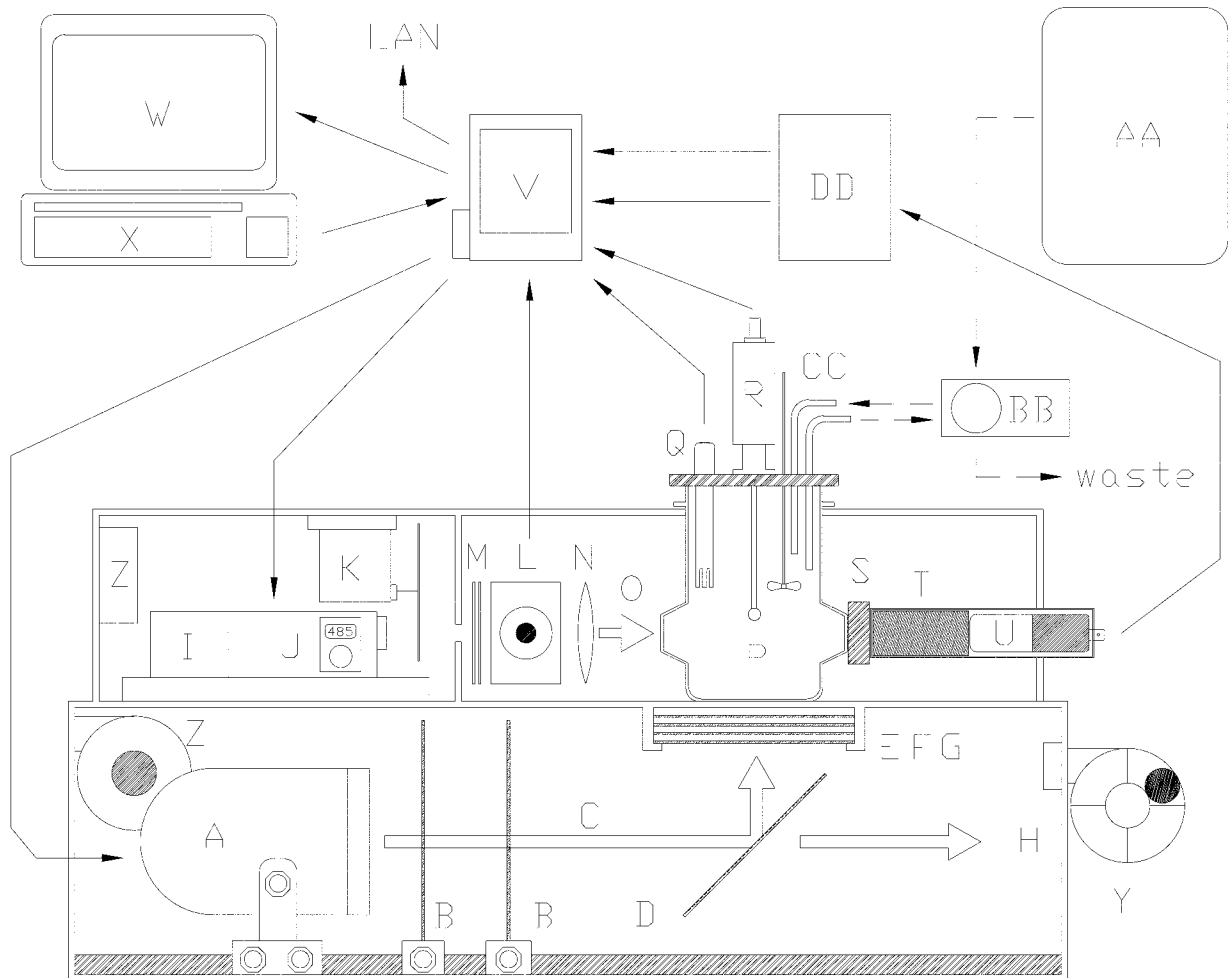
FIG. 1. Functional diagram of NFC: A—growth lamp and housing, B—Fresnel lenses, C—growth lamp output, D—cold mirror, E—heat-absorbing glass, F—blue-green bandpass filter, G—cutoff interference filter, H—IR beam dump, I—monochromator source lamp, J—mono-chromator, K—optical chopper, L—reference photodiode (behind 45° beamsplitter), M—bandpass and cutoff filters, N—lens, O—excitation beam output, P—chemostat culture vessel, Q—pH and temperature sensor, R—scalar PAR sensor, S—fluorescence emission filters, T—slit apertures, U—photomultiplier, V—single-board computer, W—video monitor, X—keyboard, Y—ventilation light trap, Z—ventilation fans, AA—media carboy, BB—manifold pump, CC—media in/out and stirring rod, DD—lock in amplifier system. Not shown: recirculating water bath, metered CO_2 supply, sample recirculating system. Thin arrows indicate direction of information flow between computer, sensors, and controls. Open arrows indicate light paths. Dashed arrows indicate flow of media.

of nutrient delivery (Kubitschek 1970), we can grow the sample culture with nutrient delivery rates that range from zero (i.e., batch mode) to any aperiodic and/or semicontinuous rate that can be programmed into the control system. An integral water jacket is connected to a recirculating water bath (Neslab RTE-211) which maintains the culture temperature at a preset level. The culture is continuously bubbled with filtered air, but since daytime photosynthesis can significantly reduce the concentration of dissolved CO_2 in the culture, a 2% CO_2 mixture is automatically metered into the culture when the pH exceeds a preprogrammed threshold. The culture is stirred continuously and kept as axenic as possible by initial sterilization, positive pressure, and submicron particulate filters on all input and output lines. The culture vessel sits inside a black aluminum

shell, which, along with dark curtains and light traps, prevents ambient room light from affecting growth of the culture.

The ambient light field in the chemostat can be manipulated with respect to both spectral distribution and intensity. A halogen light source in the base of the NFC (lamp A, Fig. 1; housing: Source 4 PAR-MCM; bulb: Ushio HPL575/115X) is dimmed or brightened by computer following a user-selected protocol. Dichroic coated lenses integral to the lamp housing remove a significant fraction of the infrared (IR) lamp output. Fresnel lenses (B, Fig. 1) external to the lamp housing focus lamp output into a series of optical filters, which selects the wavelengths that best mimic the desired visible spectrum, that is, a blue-green output with extremely little red light at the chlorophyll fluorescence wavelengths.

Reflection off a cold mirror at 90° further removes IR radiation (filter D, Fig. 1), then an IR-absorbing filter (3 mm Schott KG-3), a blue-green bandpass filter (6 mm Schott BG-39), and a 590-nm shortpass interference filter (manufacturer unknown; filters E-G, Fig. 1) select the desired visible wavelengths. This filter set can easily be modified to provide different spectral distributions. A scalar PAR sensor (R, Fig. 1; Biospherical Instruments QSL-100) is immersed in the culture to measure irradiance and provide real time feedback to the control system. Two fans (Z, Fig. 1) ventilate the inside of the NFC to remove heat from the growth lamp and the IR dump.

A recirculating system provides small volumes of phytoplankton culture to external instruments. Presently we place in line a Fast Repetition Rate fluorometer (FRRF, Chelsea Instruments Fastracka) modified with a custom flow-through cuvette in order to continuously measure variable fluorescence properties in the culture. Periodically and during calibration we add an absorption-attenuation meter (WetLabs AC9) to measure the inherent optical properties of the culture. Samples of the culture can be removed at any time for discrete analyses of properties such as pigment distribution, spectral absorption, nutrient concentration and bacterial abundance.

b. Fluorescence detection system

Two separate fluorescence signals are measured during the course of an experiment: a natural fluorescence (F_{nat}) resulting from the broadband ambient light field (lamp A, Fig. 1) and a stimulated fluorescence (F_{stim}) resulting from a weak monochromatic source (I, Fig. 1).

A photomultiplier tube (PMT: U in Fig. 1; Hamamatsu R374HA) detects the natural fluorescence emanating from the culture through a fused silica window formed into the side of the culture vessel. The PMT is oriented 90° to the growth irradiance and is preceded by a 685-nm bandpass, 30-nm full-width half-maximum interference filter (Omega Optical 685WB30), and a longpass filter (3 mm Schott RG645) to select for the wavelengths of chlorophyll fluorescence λ_{fluor} (S, Fig. 1). Two slit apertures (T, Fig. 1) limit the detector field of view to a solid angle of approximately $1.22e-2$ sr. The gain of the detector is adjusted by varying the photomultiplier dynode supply voltage.

We measure the fluorescence action spectrum in the culture vessel by stimulating fluorescence at discrete wavelength bands (typically 5-nm bandwidth) between 430 and 550 nm. Light from a halogen light source (I, Fig. 1; housing: Instruments S.A. AH10; bulb: Osram 64460) is passed through a monochromator (J, Fig. 1; Instruments S.A. H10) and then is modulated by an optical chopper (K, Fig. 1; Photon Technology Inc. OC4000) at 200 Hz. An interference filter (SWP015, manufacturer unknown) and a blue-green bandpass filter

(3 mm of Schott BG-39) further attenuate any red light in the excitation beam, minimizing cross talk between fluorescence excitation and emission. A beamsplitter directs a fraction of this excitation to a reference photodiode to monitor long-term changes in excitation intensity (L, Fig. 1). The remaining excitation (I_{mono}) is focused by a lens into the culture vessel where it stimulates a weak fluorescence signal F_{stim}. This excitation illuminates only $\approx 0.5\%$ of the culture volume and is very weak (1.8 μW at 485 nm), which in quantum units is equivalent to ≈ 0.05 μmol quanta m^{-2} s^{-1}. At this intensity, we assume that I_{mono} is too weak to generate significant physiological artifacts in measured F_{nat}.

The magnitude of measured stimulated fluorescence is comparable in magnitude to the variability in the natural fluorescence signal F_{nat}. To isolate and recover F_{stim} from the total photomultiplier output, we use a digital signal processing lock in amplifier system (LIA: DD, Fig. 1; EG & G PARC Models 181 and 7265) referenced to the optical chopper frequency. The chopping frequency of 200 Hz was chosen after examining the distribution of total system noise in the photomultiplier output in frequency space. The observation axis of the PMT and I_{mono} are not exactly collinear (offset by $\approx 166°$), which serves to minimize the detection of excitation light forward scattered by particles while maximizing the overlap between the stimulated and observed sample volumes.

c. Control and acquisition system

A single board computer on the NFC (SBC: V, Fig. 1; Ampro LittleBoard P5i) employs a data acquisition card (Computer Boards Inc. PC104/DAS16Jr) to accomplish sampling and control. This computer is integral to the NFC and is directly connected to a local area network to provide easy access to data and programs. A user interface program written in Visual C (Microsoft Corp.) contains protocols for sampling the entire suite of sensors and for manipulating key environmental parameters (e.g., temperature, pH, irradiance, and nutrient availability). Although these parameters can be adjusted by computer with a temporal resolution of 1 s, hysteresis ultimately limits the time with which adjustments to each individual parameter take effect. All analog voltage signals, including the natural fluorescence F_{nat}, are lowpass filtered with a cutoff frequency of 0.53 Hz to minimize aliasing at our sampling rate of 1 s. The voltage resolution of the analog channels is at best 0.15 mV. The stimulated fluorescence F_{stim} is digitally filtered by the lock in amplifier with a time constant of 10 s and then digitally communicated to the computer with a nominal voltage resolution of 0.1 μV.

3. Testing and evaluation

a. The ambient light field

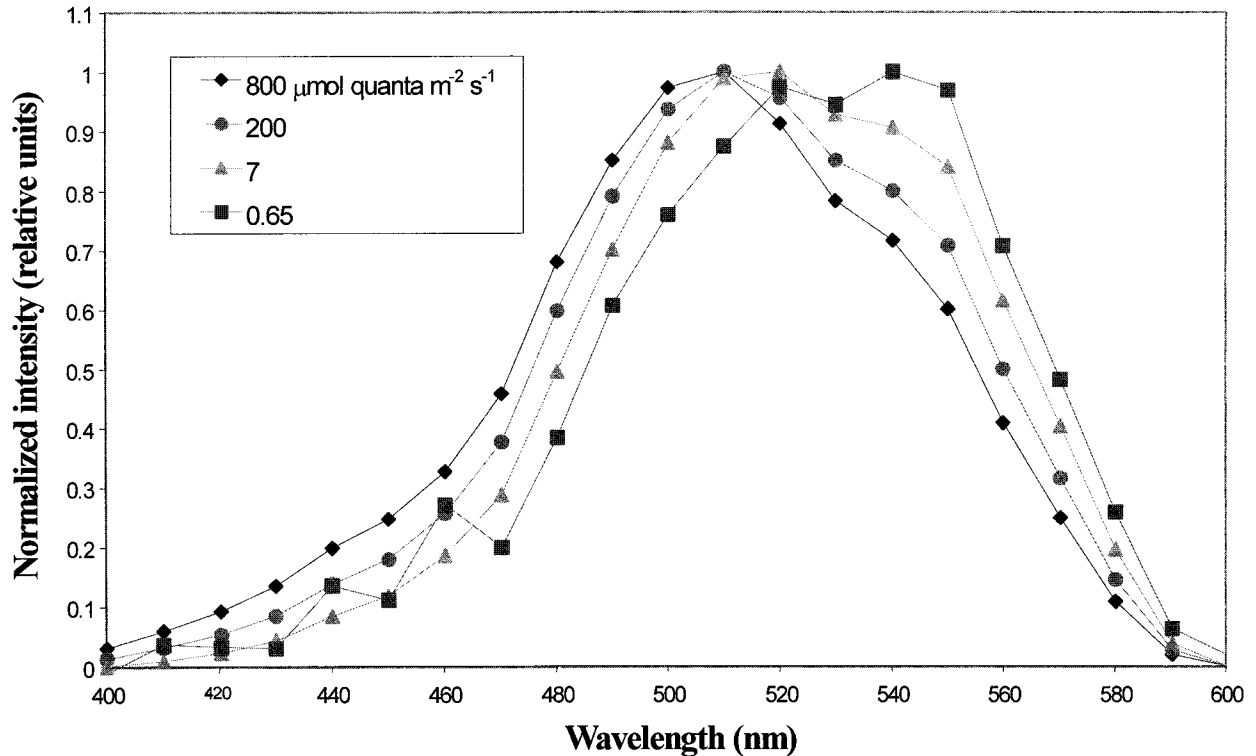The spectral character of lamps typically varies as a function of intensity. To characterize this variability we

FIG. 2. Spectral distribution of growth irradiance in the chemostat at four different intensity levels.

measured the growth light output as a function of irradiance and wavelength using a spectrometer (Ocean Optics Inc., S2000) and the integral scalar PAR sensor. Spectral data were corrected as a function of wavelength for grating efficiency and detector sensitivity, and the resulting corrected quantum spectral distribution is shown in Fig. 2 for four different irradiance levels (800, 200, 7, and 0.65 μmol quanta m^{-2} s^{-1}). The peak wavelength λ_{peak} clearly shifts toward the red as the light is dimmed, with the largest shift observed at very low irradiance levels. Although we suspect that this shift in λ_{peak} may lead to physiologically driven artifacts in F_{nat} at very low intensities, we assume that this effect is minimal in our present experiments because cultures are exposed to such low light levels for a comparatively short amount of time. However, we are mindful of this potential physiological artifact when interpreting variability in F_{nat} at very low irradiance levels.

b. Artifacts in F_{nat} measurements

Electrical noise in the sensor and electronics appears as a measurable F_{nat} in the absence of any light in the culture vessel. We measured this voltage during calibration and found it to have a mean magnitude of 0.041 mV with a distribution strongly skewed toward zero. Consequently, we estimate the inherent noise level in F_{nat} to be on the order of 0.1 mV, which is less than the voltage resolution of the analog channel measuring F_{nat}.

Consequently we neglect this source of noise in the analysis of F_{nat}.

The optical filters in the optical path of the growth lamp output remove virtually all light in the fluorescence wavelengths λ_{fluor}, which we define as the 30-nm band centered at 685 nm. We estimate that in quantum units only about 4e–10 of the ambient light field occurs within λ_{fluor} (Table 1). If one-tenth of all molecular scattering interactions in water are Raman (Mobley 1994), it can be seen from Table 1 that the majority of signal detected by the photomultiplier in the absence of particles will result from Raman scattering, given the spectral distribution of the NFC growth irradiance and the spectral transmittance of the fluorescence filters. Leakage through the emission filters at other wavelengths outside those of λ_{fluor} would contribute only a negligible amount to the total measured F'_{nat}, and consequently correction for Raman scattering must be considered first.

To obtain a correction, we measured the apparent natural fluorescence F_{nat} of growth media in the culture vessel. A prime symbol is used here to denote measurements that include or are solely composed of known artifacts. Assuming that the media has Raman scattering properties similar to those of pure seawater, F'_{nat} should be directly proportional to Raman scattering as a function of irradiance. Measurements of F'_{nat} over the irradiance range that demonstrated the most significant shift in λ_{peak} (Fig. 3; $E_{PAR} = 0.25$–75 μmol quanta m^{-2} s^{-1},

TABLE 1. A signal contamination analysis for scattered light detected by the photomultiplier. The third column "Relative scattering..." includes a scattering dependence of λ^{-4}. The fourth and fifth columns marked "Relative transmission..." and "Relative spectral..." are relative values at the PMT detection wavelengths. The final column shows the relative proportion of these scattering sources in the measured PMT output.

Wavelength of lamp output (nm)	PMT detection wavelengths (nm)	Relative proportion of photons of these wavelengths in the culture vessel	Relative scattering efficiency to get to PMT detector	Relative transmission of emission filters	Relative spectral response of PMT	Product: relative magnitude
545–565 nm: Raman excitation	670–700	≈ 0.1	≈ 0.2	1.0	1.0	0.02
670–700 nm: At chlorophyll fluorescence wavelength	670–700	4e–10	1.0	1.0	1.0	4e–10
400–700 nm: Growth light that may leak through emission filters	400–700	1.0	<10	$<10^{-8}$	<10.0	$<10^{-6}$

see Fig. 2) are well fit over this range by a linear function of irradiance E_{PAR},

$$F'_{nat} = 4.02e{-}4 E_{PAR}$$

$$+ 0.0036\, V\ (r^2 > 0.999,\ n = 13\ 001), \quad (1)$$

where E_{PAR} has the units of μmol quanta m^{-2} s^{-1}. Consequently the slope of this correction factor has units of volts per irradiance, or $V\ \mu$mol photons^{-1} m^2 s. We attribute the nonzero intercept to room light leaking into the instrument, as improved sealing resulted in undetectable F'_{nat} at E_{PAR} very near to 0. Residuals of this fit were less than 0.2 mV, comparable to the voltage resolution of the measurement channel. Given that no single measurement of F_{nat} will be resolved to better than 0.15 mV, we retain 0.4 V μmol quanta^{-1} m^2 s as the constant used to correct F'_{nat} for Raman scattering, thus yielding the actual natural fluorescence signal of interest, F_{nat}.

Another potential artifact in F'_{nat} may result from scattering of the growth irradiance by particles in the culture vessel. We estimate a worst case scenario of particle scattering using the model of Gordon and Morel (Gordon and Morel 1983), using a reference wavelength λ_{ref} of 510 nm to represent the chemostat growth irradiance
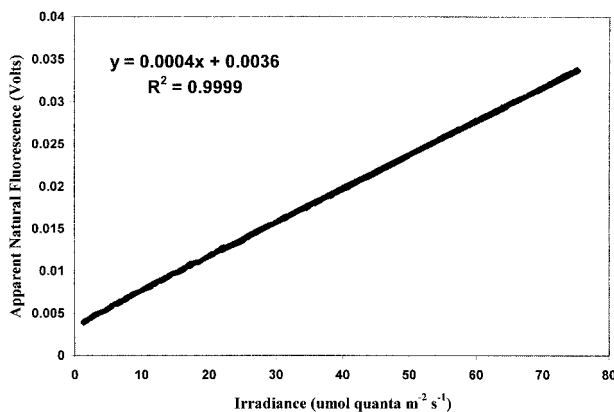

FIG. 3. Correlation between the apparent natural fluorescence of pure media and irradiance intensity.

at λ_{peak}. For this λ_{peak}, this model predicts a particulate scattering coefficient b_{part} of 5.622 m^{-1} at a chlorophyll concentration of 100 μg L^{-1}. Applying a "typical" particulate phase function (Mobley 1994), particulate scattering is 0.024 m^{-1} sr^{-1} at 90° (the observation angle of the fluorescence detector) at this unusually high chlorophyll concentration. Although the Raman scattering of quanta at this angle and wavelength is approximately three orders of magnitude smaller (1.1e$-$5 m^{-1} sr^{-1}; Bartlett et al. 1998), the fluorescence emission filters will block the particulate scattering with a much greater efficiency than the Raman scattering, approximately by a factor of 10^8. Consequently, even at these high chlorophyll concentrations Raman scattering contributes orders of magnitude more photons than elastic scattering, and so correction for total scattering using only Eq. (1) is justified.

c. Artifacts in F_{stim} measurements

Electrical noise in the room and instrument can also be observed in the F'_{stim} signal in the absence of any source of light. We measured this noise during calibration and found it to have a mean magnitude of 11.5 μV and to be normally distributed with a standard deviation of 2.13 μV. Using three standard deviations above mean to represent the noise floor, we estimate the lowest detectable F_{stim} to be around 18 μV. This level is significant compared to the nominal voltage resolution of this measurement and so we correct for this instrument noise in our analysis of F_{stim}.

Apparent stimulated fluorescence F'_{stim} can also include artifacts due to a combination of Raman, molecular, and particulate scattering of growth irradiance. Since the detector sensitivity and the optical geometry for F_{stim} vary with excitation wavelength, the relative magnitudes of these artifacts in F'_{stim} may be different than those in F'_{nat}. Measurements of F_{stim} are used at present only for long-term comparisons on the order of days, and so we can limit our discussion of the scattering error in F'_{stim} to measurements collected only during sim-

ulated nighttime, when no irradiance-dependent scattering occurs.

To correct for molecular scattering, we measured the apparent stimulated fluorescence F'_{stim} of pure media with the growth lamp off. At an excitation wavelength λ_{mono} of 485 nm, F'_{stim} had a mean magnitude of 10.6 μV and substantial variability ($\sigma = 2.4$ μV, $n = 3965$). Using a series of short pass and long pass interference filters at different locations in the optical train, we determined that this signal was due primarily to scattered excitation light, which generated fluorescence in the emission filters. This signal is small compared to the magnitude of F'_{stim} measured in the presence of phytoplankton, but we incorporate it as a correction for completeness.

Particulate scattering may have a larger influence on F'_{stim} than F'_{nat} because enhanced scattering of particles at forward angles may be detected by the PMT due to the nearly collinear geometry of the optical train. We again use Gordon and Morel's model to calculate a worst case scattering coefficient of 5.91 m^{-1} for a culture of 100 μg L^{-1} of chlorophyll at $\lambda = 485$ nm. The photomultiplier observes a field 2.8° wide in the horizontal, offset by 14° from the direction of beam travel (i.e., 166° from the horizontal axis of the beam). Using again a "typical" phase function value at 14° of 0.4893 sr^{-1}, the volume-scattering function of the excitation beam at 14°, $\beta_{part}(14°)$, is 2.89 m^{-1} sr^{-1}. Since the particulate scattering is generated along the path of the excitation beam, $\beta_{part}(14°)$ in this geometry also describes the relationship between incident irradiance and the resulting scattered radiance per unit pathlength into an angle 14° from the direction of propagation. Since the solid angle of the detector and the pathlength of travel through the culture vessel are known, multiplying $\beta_{part}(14°)$ by these values provides a rough estimate of the fraction of the excitation beam scattered by particles into the photomultiplier field of view. We calculate this ratio to be 3.4e–3.

Since the monochromator output intensity is known (1.8 μW at $\lambda = 485$ nm), the optical power scattered into the photomultiplier field of view by particles is then approximately 7.2 nW. The fluorescence emission filters will attenuate light at this wavelength by at least 10^{-8}, which reduces this signal to $\approx 7e-17$ W. The anode radiant sensitivity of this photomultiplier (3.4e4 A W^{-1}) and the subsequent current to voltage gain of the lock in amplifier system (typically 10^{-6} A V^{-1}) are insufficient to amplify this signal to levels detectable above the F_{stim} channel instrument noise. Consequently, particulate scattering is considered negligible with respect to the measured stimulated fluorescence F'_{stim} at any wavelength in the visible spectrum.

d. Artifacts in fluorescence action spectra

To construct a fluorescence action spectrum, the center wavelength of the F_{stim} excitation source is periodically scanned between 430 and 550 nm in 5-nm increments. We measured the apparent stimulated fluorescence F'_{stim} between $\lambda = 400$ and 750 nm in pure water as a function of wavelength and observed three distinct peaks (Fig. 4). Analysis of these peaks upon insertion of longpass and shortpass interference filters at key points in the optical path indicated that the peak centered around 550 nm is due to the excitation of Raman scattering of water into the fluorescence signal wavelengths λ_{fluor}. The broader peak around 470 nm appears to result from filter fluorescence in the PMT emission filters. The small peak around 680 nm shows direct coupling of I_{mono} into the detector due to forward scattering by water, which can be ignored as measurement of F_{stim} occurs only with excitation wavelengths between 430 and 550 nm. The intensity of I_{mono} is not constant between 430 and 550 nm, because the throughput efficiency and the output of monochromator source lamp are not constant as a function of wavelength. However, I_{mono} is measured constantly by the reference photodiode, and consequently F'_{stim} can be corrected between 430 and 550 nm for Raman scattering and filter fluorescence using the data in Fig. 4 and the reference diode voltage.

4. Live culture data

Using the NFC we have collected several natural fluorescence time series with different species of phytoplankton under various environmental conditions. As an example, a 45-day series of F_{nat} from a highly concentrated culture of the marine diatom *T. weissflogii* (Bacillariophyceae) is shown in Fig. 5a. Irradiance was modeled in this experiment as a sinusoid, with a daily maximum of 75 μmol quanta m^{-2} s^{-1} and a 12:12 light–dark cycle. A programming error in the lamp control routine led to a short period of nonsinusoidal irradiance on day 224. The maximum chlorophyll concentration in the culture vessel during these 45 days was 130 μg L^{-1}, and although such high chlorophyll concentrations are rarely found in nature, these preliminary results allow patterns in F_{nat} to be more easily identified for later comparison with dilute cultures.

Natural fluorescence is a strong function of instantaneous irradiance, and so to remove irradiance as a source of variability we calculate the coefficient of fluorescence $\Phi(\lambda_F, \lambda_E)$ as $F_{nat}(E_{PAR})^{-1}$, following Gordon (1979). We used this coefficient as a proxy for fluorescence quantum efficiency $\eta(\lambda_F, \lambda_E)$ because we do not measure phytoplankton absorption as a function of wavelength and therefore cannot calculate the actual quantum efficiency. However, no significant variability in the fluorescence action spectrum was observed during this period and so we make the simplifying assumption that phytoplankton spectral absorption varies little and thus $\Phi(\lambda_F, \lambda_E)$ to the first order estimates $\eta(\lambda_F, \lambda_E)$.

Over these 45 days the gross trend in both F_{nat} and $\Phi(\lambda_F, \lambda_E)$ reflects changes in the culture chlorophyll concentration [chl *a*] (Figs. 5a,b). However, during this
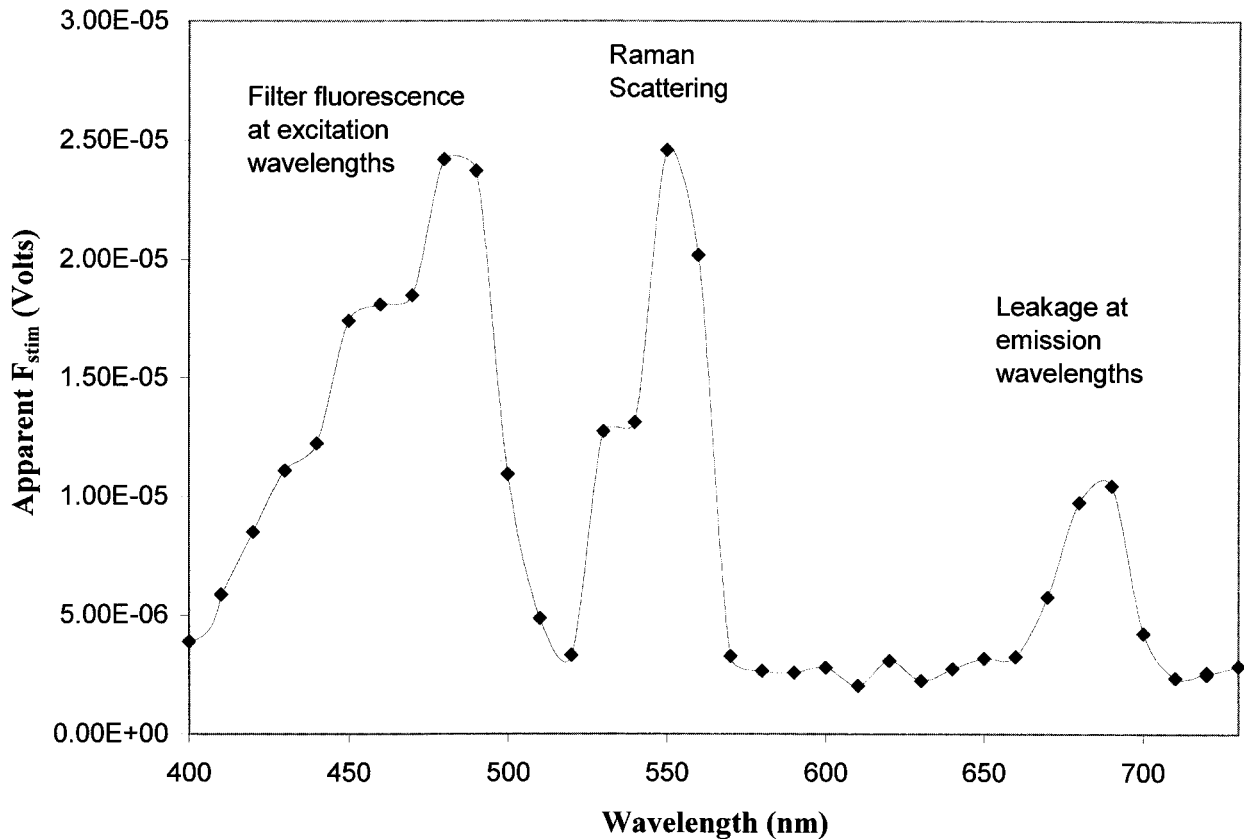
FIG. 4. Apparent weak stimulated fluorescence F'_{stim} of pure water as a function of excitation wavelength. The peaks at 480, 550, and 685 nm, respectively, result from filter fluorescence, Raman emission, and direct coupling between the monochromator output and the detector.

period the relationship between culture chlorophyll and $\Phi(\lambda_F, \lambda_E)$ varies substantially (Fig. 6), indicating irradiance independent variability in F_{nat}. Each datum in Fig. 6 shows the relationship between $\Phi(\lambda_F, \lambda_E)$ at solar noon and predawn [chl a] for days between 222 and 256 (missing day 255), and there is no significant correlation between these variables ($r^2 = 0.57$, $n = 33$). During the initial 12 days of exponential growth (chlorophyll growth rate = 0.16 day^{-1}, $r^2 > 0.98$, $n = 4$), there appears to be a constant relationship between [chl a] and $\Phi(\lambda_F, \lambda_E)$ (drawn explicitly in Fig. 6 as line I, open circles). After this period of exponential growth, the relationship between [chl a] and $\Phi(\lambda_F, \lambda_E)$ becomes more variable, but we identified two trends that indicate this relationship is not due to random processes.

First, $\Phi(\lambda_F, \lambda_E)$ appears to increase independently of [chl a] after introducing a small amount of antibiotic. Twice during this experiment (evening of day 223 and morning of day 240), 10 mL of a dilute erythromycin solution was added to the culture in order to evaluate its potential use for controlling bacterial contamination. Although there is no change in the F_{nat} signal within 24 h after these additions (Fig. 6, closed triangle and square for day 224 and 240, respectively), $\Phi(\lambda_F, \lambda_E)$ clearly increases over 4 days following each addition (Fig. 6, open triangles and squares). Since the antibiotic solution

exhibited no measurable signal in the chlorophyll fluorescence wavelengths (Turner Designs AU-10) and since F_{nat} did not increase immediately with the additions, we discount the possibility that the antibiotic solution contributes directly to the increase in $\Phi(\lambda_F, \lambda_E)$. Even though we did not perform a control addition of distilled water at another time during the experiment, we suspect that the observed increases in $\Phi(\lambda_F, \lambda_E)$ after each addition reflect a physiological response to the antibiotic by the culture phytoplankton. This response may be directly caused by the antibiotic (i.e., a physiological reaction to the presence of the antibiotic) or indirectly caused (e.g., due to an increase in available nutrients from a declining bacterial population), but for our purposes the underlying mechanism is less important than the observation that chlorophyll- and irradiance-independent variability in $\Phi(\lambda_F, \lambda_E)$ can indicate physiological response to a specific environmental disturbance.

A second pattern becomes apparent when the data representing these erythromycin treatments are removed. Diamond symbols in Fig. 6 represent days 223–256 and exclude the two 5-day periods of erythromycin treatment. These data fall into two groups: a general linear trend indicated by line II and a small group of outliers indicated by open diamond symbols. Ignoring the outliers, the correlation between [chl a] and $\Phi(\lambda_F,$
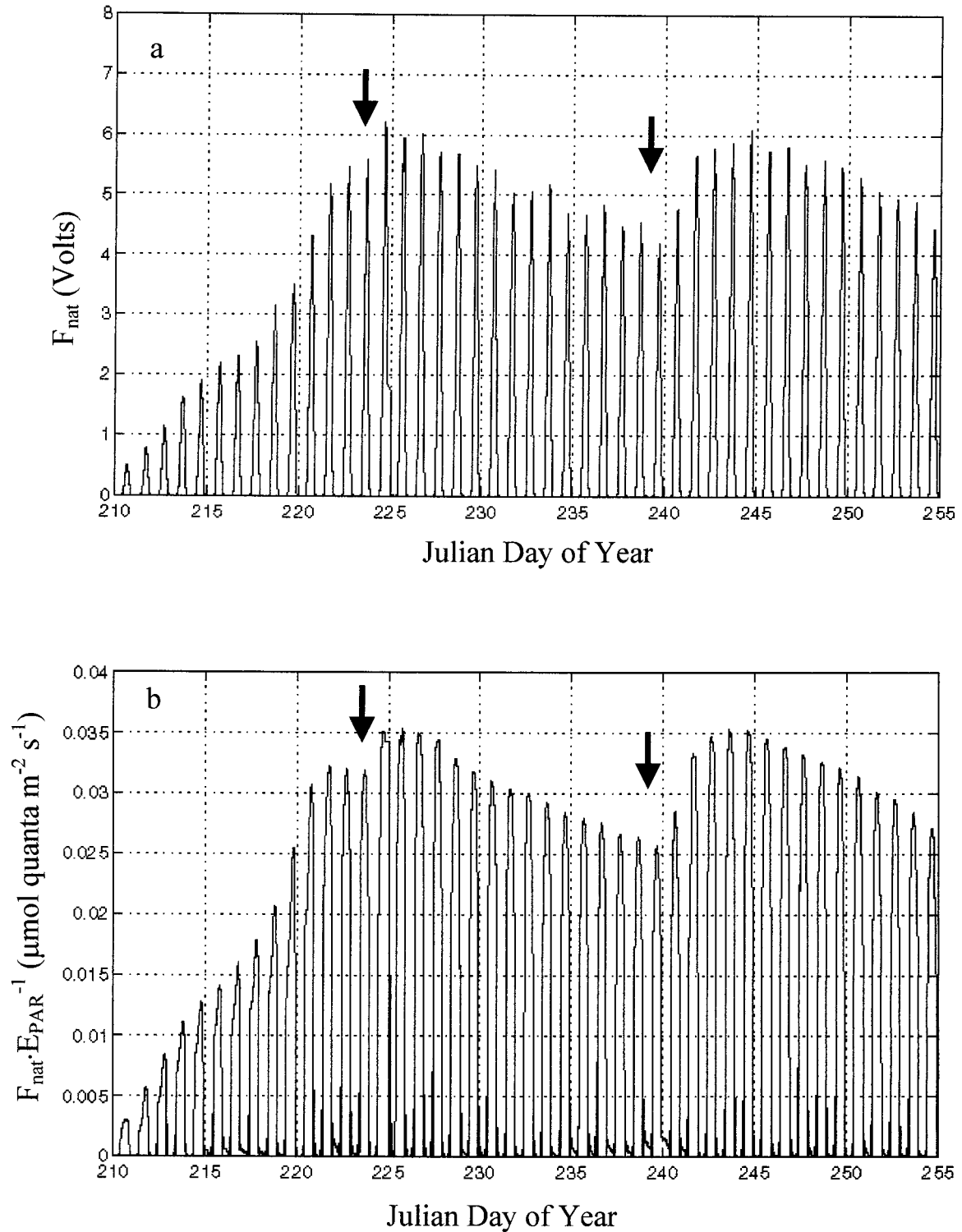
FIG. 5. (a) Natural fluorescence signal F_{nat} vs Julian day. Although diurnal irradiance (E_{PAR}) is sinusoidal, diurnal F_{nat} is not. (b) F_{nat} normalized to E_{PAR} with 1-s resolution. Addition of dilute erythromycin solution in the evening of day 223 and morning of day 240 is noted by arrows.
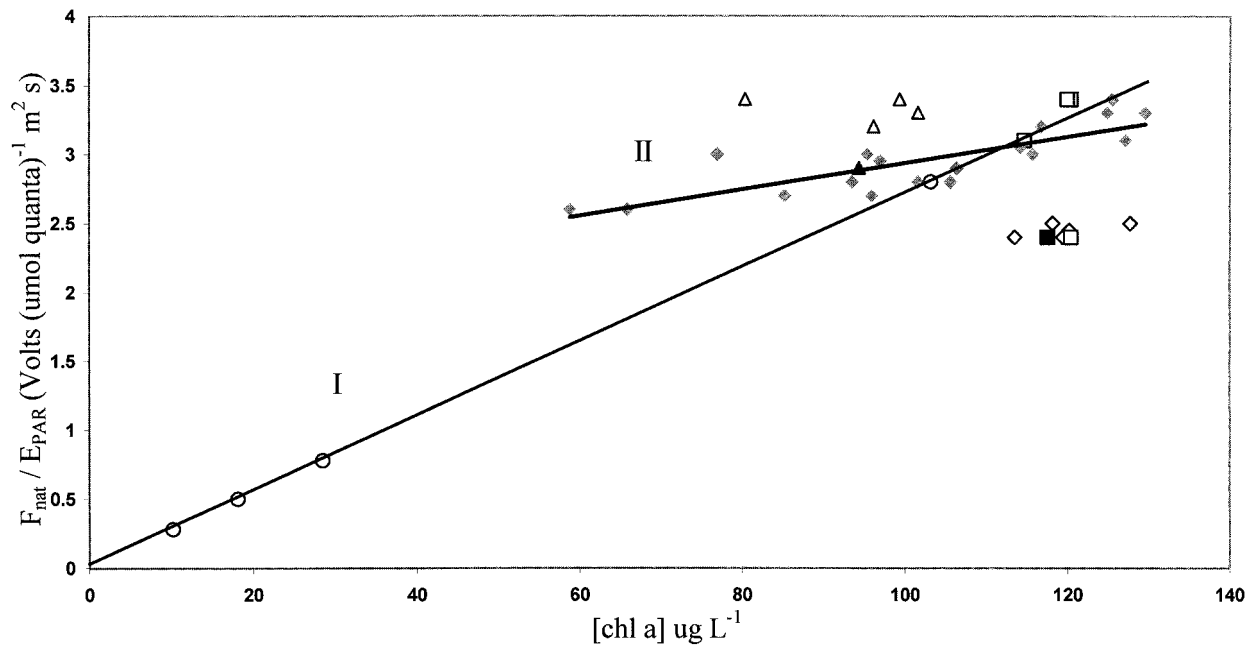
FIG. 6. Scatterplots of $F_{nat} (E_{PAR})^{-1}$ as a function of chlorophyll concentration. Line I denotes initial exponential growth (open circles: days 211–213, 222). The two periods following erythromycin addition are shown as triangles and squares, respectively, closed symbols representing the day of the treatment and open symbols representing four subsequent days following each. Diamond symbols represent the remaining days, open diamonds indicate relatively steady-state growth, and line II indicates the regression through the closed diamond symbols only.

λ_E) is only slightly stronger than that for the entire dataset ($r^2 = 0.68$, $n = 18$), but the slope of this relationship is much less than that of the exponential growth phase. In general, $\Phi(\lambda_F, \lambda_E)$ appears to be proportionally higher than [chl a] for this subset of data, and we suggest that the relative increase in $\Phi(\lambda_F, \lambda_E)$ may indicate a transition from exponential growth toward steady state in the culture vessel. The second group (Fig. 6, open diamonds) are tightly packed well below the regression line and represent two distinct periods: days 236–238 and 254–256. From Fig. 5 it can be seen that these periods occur 8–10 days after each erythromycin addition, when cell counts and extracted chlorophyll measurements show relative constancy (data not shown). Our initial interpretation of this distribution is that the second group reflects relatively steady-state growth in the culture, and perhaps would be the region in [chl a] $-$ $\Phi(\lambda_F, \lambda_E)$ space to where an undisturbed culture of *T. weissflogii* grown under these conditions would converge.

We are presently analyzing nutrient, pigment, and FRRF variable fluorescence data from this preliminary experiment and others to further investigate variability in the relationship between [chl a] and $\Phi(\lambda_F, \lambda_E)$ in phytoplankton. Although the physiological mechanisms that control this relationship are not well understood, the natural fluorescence signal appears to contain information regarding culture response to disturbances in the chemical environment, in addition to information associated with relative growth rate. Although a quan-

titative assessment may be unfeasible, even for a single species, qualitative interpretation of variability in the relationship between [chl a] and $\Phi(\lambda_F, \lambda_E)$ may provide a means to better understand observed variability in field measurements of sun-stimulated fluorescence.

5. Summary

These time series data represent the first detailed look into the physiological variability of natural fluorescence, that is, the variability in F_{nat} not accounted for by the instantaneous irradiance and chlorophyll concentration. Using the developed NFC system, most of the environmental factors known to influence phytoplankton natural fluorescence can be manipulated independently, allowing the influence of each on F_{nat} to be quantitatively assessed in controlled phytoplankton cultures. The ability to measure F_{nat} under high irradiance conditions allows for examination of natural fluorescence at the intensities commonly encountered in the surface ocean. Simultaneous measurement of the fluorescence action spectrum provides a means to correlate observed variability in natural fluorescence with specific changes in phytoplankton spectral absorption. Experiments using laboratory instruments such as the NFC can help to explore the much needed causative relationships between environmental factors and sun-stimulated fluorescence.

While developing and evaluating the NFC several issues were raised for later improvement. Although the

theoretical and observational scattering arguments presented here may be sufficient for initial evaluation, a more direct method to assess the scattering contribution to F'_{nat} would be valuable. We are experimenting with a calibration protocol that uses additional emission filters to measure scattering at wavelengths near to but not at λ_{fluor}. Second, extending the maximum irradiance intensity in the culture vessel to over 2000 μmol quanta m^{-2} s^{-1} would more completely mimic the intensities encountered in the surface ocean. Third, it appears that reducing emission filter fluorescence would substantially improve not only measurement of F_{stim} but of F_{nat} as well, and alternate emission filter combinations are presently being evaluated for this purpose.

REFERENCES

Abbott, M. R., and R. M. Letelier, 1997a: Bio-optical drifters—Scales of variability of chlorophyll and fluorescence. *Soc. Photo-Opt. Instrum. Eng.,* **2963,** 216–221.

——, and ——, 1997b: Going with the flow—The use of optical drifters to study phytoplankton dynamics. *Monitoring Algal Blooms: New Techniques for Detecting Large-Scale Environmental Changes,* M. Kahru and C. W. Brown, Eds., Landes Bioscience, 143–168.

——, and ——, 1998: Decorrelation scales of chlorophyll as observed from bio-optical drifters in the California Current. *Deep-Sea Res. II,* **45,** 1639–1667.

——, ——, S. R. Laney, and J. S. Bartlett, 2000: Field and laboratory measurements of passive fluorescence and applications to MODIS data. *Proc. Ocean Optics XV,* Monaco, CD-ROM.

Bartlett, J. S., K. J. Voss, S. Sathyendranath, and A. Vodacek, 1998: Raman scattering by pure water and seawater. *Appl. Opt.,* **37,** 3324–3332.

Chamberlin, S., and J. Marra, 1992: Estimation of photosynthetic rates from measurements of natural fluorescence: Analysis of the effects of light and temperature. *Deep-Sea Res.,* **39,** 1695–1706.

——, C. R. Booth, D. A. Kiefer, J. H. Morrow, and R. C. Murphy, 1990: Evidence for a simple relationship between natural fluorescence, photosynthesis and chlorophyll in the sea. *Deep-Sea Res.,* **37,** 951–973.

Cullen, J. J., and M. R. Lewis, 1995: Biological processes and optical measurements near the sea surface: Some issues relevant to remote sensing. *J. Geophys. Res.,* **100,** 13 255–13 266.

Doerffer, R., 1993: Estimation of primary production by observation of solar-stimulated fluorescence. *ICES Mar. Sci. Symp.,* **197,** 104–113.

Gordon, H. R., 1979: Diffuse reflectance of the ocean: The theory of its augmentation by chlorophyll *a* fluorescence at 685 nm. *Appl. Opt.,* **18,** 1161–1166.

——, and A. Morel, 1983: *Remote Assessment of Ocean Color for Interpretation of Satellite Visible Imagery: A Review.* Coastal and Estuarine Studies, Vol. 4, Springer-Verlag, 114 pp.

Hu, C., and K. J. Voss, 1998: Measurement of solar-stimulated fluorescence in natural waters. *Limnol. Oceanogr.,* **43,** 1198–1206.

Kiefer, D. A., and R. A. Reynolds, 1992: Advances in understanding phytoplankton fluorescence and photosynthesis. *Primary Productivity and Biogeochemical Cycles in the Sea,* P. G. Falkowski and A. D. Woodhead, Eds., Plenum Press, 155–174.

——, W. S. Chamberlin, and C. R. Booth, 1989: Natural fluorescence of chlorophyll a: Relationship to photosynthesis and chlorophyll concentration in the western South Pacific gyre. *Limnol. Oceanogr.,* **34,** 868–881.

Kubitschek, H. E., 1970: *Introduction to Research with Continuous Cultures.* Prentice-Hall Inc., 195 pp.

Letelier, R. M., and M. R. Abbott, 1996: An analysis of chlorophyll fluorescence algorithms for the Moderate Resolution Imaging Spectrometer (MODIS). *Remote Sens. Environ.,* **58,** 215–223.

——, ——, and D. M. Karl, 1997: Chlorophyll natural fluorescence response to upwelling events in the Southern Ocean. *Geophys. Res. Lett.,* **24,** 409–412.

Mobley, C. D., 1994: *Light and Water, Radiative Transfer in Natural Waters.* Academic Press, 594 pp.

Stegmann, P. M., M. R. Lewis, C. O. Davis, and J. J. Cullen, 1992: Primary production estimates from recordings of solar-stimulated fluorescence in the equatorial Pacific at 150 degrees W. *J. Geophys. Res.,* **97** (C1), 627–638.